Nonlinear Quantum Optics with Rydberg Atoms

Nathan C. Song
Department of Physics, University of California, Berkeley and
Challenge Institute for Quantum Computation, University of California, Berkeley
(Dated: May 10, 2024)

In this review paper, we explore how electromagnetically induced transparency (EIT) and Rydberg interactions create nonlinear optical effects. We begin by dissecting the Hamiltonian for a 'L'-type three-level atomic system, and show how EIT arises. We then go over a derivation of the nonlinear susceptibility [1] and introduce Rydberg interactions to the 'L'-type Hamiltonian. We then expand from a single Rydberg atom to an ensemble of Rydberg atoms to examine the Rydberg superatom [2] and quantum metasurfaces [3]. Applications of these ideas for single photon sources [4] and generating highly entangled photon states [3, 5] are then explored.

I. INTRODUCTION

Electromagnetically induced transparency and Rydberg interactions have been well explored in the past decades [2, 6–8], yet an abundance of new ideas and experimental results are being produced to this day [9–11]. Applications are widespread, including but not limited to atomic clocks [9], spectroscopy [12], quantum metamaterials [3], slow light [13, 14], and photonic molecules in Rydberg atom ensembles [15]. As such it is important to understand how EIT creates tunable nonlinear susceptibilities in three-level atoms, and how Rydberg interactions modify or amplify these susceptibilities.

With recent progress on using Rydberg atoms for the purposes of quantum simulation [16, 17], understanding the nonlinearities that EIT and Rydberg interactions create is doubly important. Nonlinear effects allow for the generation of single photons [4], a coherent transfer of information from the energy levels of a Rydberg atom to a photonic state [15], and fluorescence imaging of single atoms [18]. Each of these usages are important for near-term fault tolerance [7] . Furthermore, the development of ideas like Rydberg superatoms have opened the floor to a new kind of qubit. As opposed to storing a qubit on a single atom or even a logical qubit based on multiple individual atoms, qubits stored on a Rydberg superatom may provide a robust, long-lived alternative option [11].

In this review paper, we present a coherent explanation of the nonlinearities produced by EIT and Rydberg interactions. At their core, EIT and Rydberg interactions are simple effects. Transparency in a three-level atomic system comes from the existence of a 'dark state' that is unaffected by resonant drive fields due to constructive interference. Rydberg blockade comes from the induced energy shift of a dipole from another dipole, which shifts the transition from a ground to Rydberg state off-resonance. However, topics like the nonlinear susceptibility of a material, Rydberg superatoms, and quantum metasurfaces are much more challenging. In the following sections we will present a broad introduction to EIT, the Rydberg interaction, and the aforementioned topics.

II. BACKGROUND

In Rydberg atoms, nonlinear effects in the few-photon regime can be induced through electromagnetically induced transparency (EIT) or dipole-dipole interactions (commonly known as Rydberg interactions) between excited atoms. In this section we show how the Hamiltonian of a three-level system driven by two electromagnetic fields in an 'L' type configuration allows for a special 'dark-state' that is transparent to incoming resonant light. We then formally introduce the Rydberg interaction, and proceed to examine how EIT and Rydberg interactions can effectively create a tunable nonlinear susceptibility in a single atom.

A. EIT in Three-Level Atomic Systems

Electromagnetically induced transparency can be found in any three-level atomic system with a two-photon transition. Two examples of such systems, dubbed 'λ' and 'L' structures, are illustrated in Figure 1. As many derivations for EIT in a 'λ' type system can be found elsewhere [8, 19], we will provide one only for the 'L' setup. The derivation is nearly identical to that of the 'λ' setup. Begin by writing the Hamiltonian for the 'L' setup:

$$\begin{aligned} H &= \hbar\omega_0|0\rangle\langle 0| + \hbar\omega_1|1\rangle\langle 1| + \hbar\omega_r|r\rangle\langle r| \\ &+\frac{\hbar}{2}(\Omega_{hf}e^{-i\omega_{01}t}|1\rangle\langle 0| + \Omega_r e^{-i\omega_{1r}t}|r\rangle\langle 1| + h.c.), \end{aligned} \tag{1}$$

where $\hbar\omega_j$ is the energy corresponding to each state and Ω_{hf}, Ω_r are the Rabi oscillation frequencies for each input field. Our goal is to remove the time-dependent components of this Hamiltonian, which we can do by applying the RWA (Rotating Wave Approximation) in the same fashion as section 1.6.3 in [20]. We seek to find some $U(t)$ such that $|\psi\rangle_{IP} = U(t)|\psi\rangle$, or equivalently

$$H_{IP} = U(t)HU^\dagger(t) + i\hbar U(t)\partial_t U^\dagger(t) \tag{2}$$

We can then write $U = \sum_j e^{-i\lambda_j t}|j\rangle\langle j|$ for some cur-

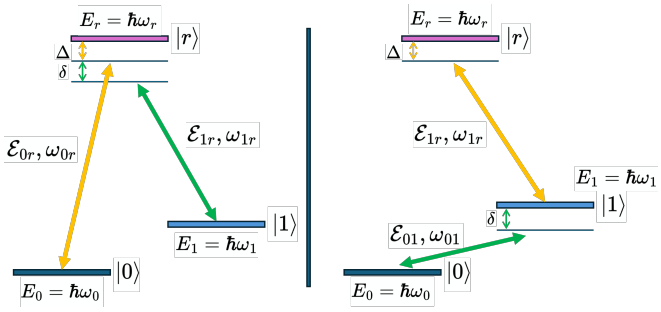

FIG. 1. Left: A 'λ' setup where two hyperfine states are each coupled to an excited (Rydberg) state. Δ and δ are the detunings of the drive lasers. $\mathcal{E}_{0r}$, $\mathcal{E}_{1r}$ and ω_{0r}, ω_{1r} are the amplitude and frequency of the drive lasers from the $|0\rangle$ to $|r\rangle$ and $|1\rangle$ to $|r\rangle$ respectively. $E_j = \hbar\omega_j$ is the energy corresponding to each state. Right: An 'L' setup where the two hyperfine states are coupled to each other, and only the $|1\rangle$ state is coupled to an excited (Rydberg) state.

rently unknown λ_j, where $j \in \{0, 1, r\}$. Then

$$H_{IP} = \hbar \begin{pmatrix} \omega_0 - \lambda_0 & \frac{\Omega_{hf}^*}{2} e^{-iAt} & 0 \\ \frac{\Omega_{hf}}{2} e^{iAt} & \omega_1 - \lambda_1 & \frac{\Omega_r^*}{2} e^{-iBt} \\ 0 & \frac{\Omega_r}{2} e^{iBt} & \omega_r - \lambda_r \end{pmatrix}, \tag{3}$$

where we write $A = -\lambda_0 - \omega_{01} + \lambda_1$ and $B = -\lambda_1 - \omega_{1r} + \lambda_r$. To remove time-dependence from H_{IP} then, we must simultaneously satisfy the following conditions (The first condition is set merely to simplify our Hamiltonian):

$$\begin{aligned} \omega_0 - \lambda_0 &= 0, \\ \lambda_0 + \omega_{01} - \lambda_1 &= 0 \\ \lambda_1 + \omega_{1r} - \lambda_r &= 0. \end{aligned} \tag{4}$$

Solving this system of equations reveals that $\omega_1 - \lambda_1 = \delta$ and $\omega_r - \lambda_r = -\Delta + \delta$. And so,

$$H_{IP} \to \hbar \begin{pmatrix} 0 & \frac{\Omega_{hf}^*}{2} & 0 \\ \frac{\Omega_{hf}}{2} & \delta & \frac{\Omega_r^*}{2} \\ 0 & \frac{\Omega_r}{2} & \delta - \Delta \end{pmatrix}. \tag{5}$$

We can then find the eigenstates of this Hamiltonian for the two-photon resonance case where $\Delta = \delta$:

$$\begin{aligned} |a^+\rangle &= \frac{1}{A}\left(\frac{\Omega_{hf}}{\Omega_r}|0\rangle + \frac{\delta - \sqrt{\Omega_{hf}^2 + \Omega_r^2 + \delta^2}}{\Omega_r}|1\rangle + |r\rangle\right) \\ |a^0\rangle &= \frac{1}{\sqrt{\Omega_r^2 + \Omega_{hf}^2}}(-\Omega_{hf}|0\rangle + \Omega_r|r\rangle) \\ |a^-\rangle &= \frac{1}{B}\left(\frac{\Omega_{hf}}{\Omega_r}|0\rangle + \frac{\delta + \sqrt{\Omega_{hf}^2 + \Omega_r^2 + \delta^2}}{\Omega_r}|1\rangle + |r\rangle\right], \end{aligned} \tag{6}$$

where A and B are normalization factors. These eigenstates correspond to the following eigenvalues

$$\begin{aligned} \lambda_+ &= \frac{\hbar}{2A}(\omega - \sqrt{\Omega_{hf}^2 + \Omega_r^2 + \delta^2}) \\ \lambda_0 &= 0 \\ \lambda_- &= \frac{\hbar}{2B}(\omega + \sqrt{\Omega_{hf}^2 + \Omega_r^2 + \delta^2}). \end{aligned} \tag{7}$$

Examining the eigenvalues of our 'L' type configuration we can now see proof of EIT. The eigenvector corresponding to an eigenvalue of 0,

$$|a^0\rangle = \frac{1}{\sqrt{\Omega_r^2 + \Omega_{hf}^2}}(\Omega_{hf}|0\rangle - \Omega_r|r\rangle), \tag{8}$$

is an invariant 'dark state'. As there is no probability of $|a^0\rangle$ being in the Rydberg state $|r\rangle$, $|a^0\rangle$ remains unchanged under any resonant drive field. This invariance means that the 'dark state' atom is effectively transparent to any resonant laser light due to destructive interference, as there is no possibility of spontaneous emission from an excited state.

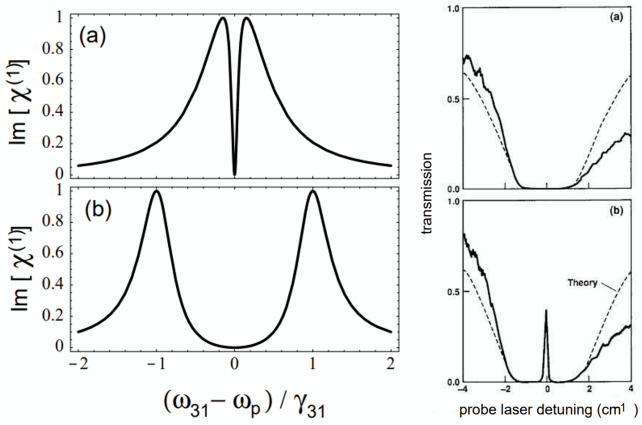

FIG. 2. **Left:** Numerical calculations of the EIT absorption spectrum [8] for different coupling field strengths. The y-axis shows the imaginary component of the linear susceptibility of a three-level atom in a 'λ' setup. (a) is for $\Omega_c = 0.3\gamma_{31}$, and (b) shows $\Omega_c = 2\gamma_{31}$. The coefficients here represent the $|0\rangle, |1\rangle, |r\rangle$ states as 0, 1, and 3 respectively, with $\Omega_c \to \Omega_r$. **Right:** Plots from first experimental demonstration of EIT [21]. The top plot shows transmission through a Sr vapor cell without the coupling field on, the bottom plot shows transmission with the coupling field on.

If we proceeded to solve the master equations for this setup, we would obtain a relation for the linear susceptibility of this setup and obtain a graph similar to Figure 2 [8]. Figure 2 shows the EIT absorption spectrum for different values of coupling fields in a 'λ' setup and a graph showing an experimental realization of EIT.

Tracking the imaginary part of the linear susceptibility (Figure 2a), we can see that the transparency window corresponding to the 'dark state' of the 'λ' system at

$(\omega_{31} - \omega_p)/\gamma_{31} = 0$ corresponds to the peak in the transmission graph on the right. This is experimental confirmation that a three-level atom can be made transparent to resonant laser light. Another interesting feature of the nonlinear susceptibility is its tunability: by increasing the magnitude of Ω_c, the the EIT transparency window can be widened. This feature, along with a proper derivation of the nonlinear susceptibility of our 'L' configuration, will be discussed in section C.

B. The Rydberg Interaction

While the derivation above explains how EIT arises in a three-level 'L' setup, it does not include a term for Rydberg interactions. Rydberg interactions occur because an atom in the strongly excited Rydberg state $|r\rangle$ creates a dipole moment so potent that the electric field it generates detunes the transition frequency to the Rydberg state for nearby atoms. As such, addressing an atom (atom A) spatially close (see Figure 3) to another atom (atom B) in the state $|r\rangle$ with laser light initially resonant with the Ω_{1r} or Ω_{0r} transition no longer affects the populations of the system state. This is because the energy spectrum of atom A has been altered so strongly by atom B that our addressing laser light is no longer on resonance. This example of complete blockage from an excited atom B of atom A from accessing the Rydberg state is aptly called the Rydberg blockade effect.

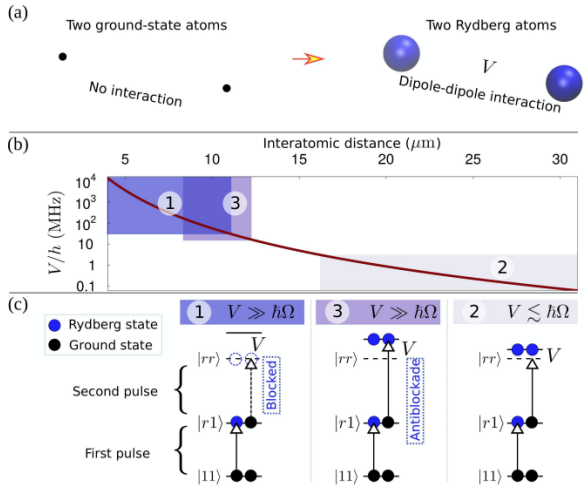

FIG. 3. Figure from [22]. (a) A cartoon image of two Rydberg atoms as opposed to two ground-state atoms, with the increased size of the Rydberg atoms suggestive of their larger electron orbital radius. (b) A graph of the interaction potential vs. distance with different interaction regimes labeled. (c) Diagrams of interaction regimes. 1. Rydberg blockade effect within the critical radius. 2. Weak interaction potential in which a second Rydberg atom can be excited, but a dynamic phase can arise due to the interaction between two excited dipoles. 3. Intermediate interaction potential in which Rydberg excitations are antiblockaded.

As shown in Figure 3, this complete blockage is found when our Rydberg atoms are within a certain distance of one another. In the case of Rubidium with $|r\rangle$ chosen as the s-orbital of principal quantum number 100 ($100S_{1/2}$), this strong-interaction regime can be found for two atoms within $11\mu m$ of each other. This value of $11\mu m$ is then our Rydberg blockade radius. In weaker regimes for larger atom separations (Cases 2 and 3 in Figure 2), the Rydberg interaction can still act as a generator of entanglement between neighboring atoms.

As the interaction of two Rydberg atoms is a dipole-dipole interaction, a Van-der Waals potential is generated between two atoms in the $|r\rangle$ state:

$$V = \frac{C_6}{|\vec{x}_j - \vec{x}_k|^6}, \tag{9}$$

where the interaction strength C_6 is determined by the specifics of the Rydberg state dipole moment. For a system of multiple Rydberg atoms placed in free space, then, we can write the full Hamiltonian for an 'L' type setup:

$$\begin{aligned} H(t)/\hbar = \sum_i \frac{\Omega_i^{hf}(t)}{2}(e^{i\omega_{01}^i(t)}|0_i\rangle\langle 1_i| + h.c.) \\ - \sum_i \Delta_i^{hf}(t)|1_i\rangle\langle 1_i| + \sum_i \frac{\Omega_i^r(t)}{2}(e^{i\omega_{1r}^i(t)}|1_i\rangle\langle r_i| + h.c.), \\ - \sum_i [\Delta_i^{hf} + \Delta_i^r]|r_i\rangle\langle r_i| + \sum_{i<j} V_{ij}|r_i\rangle\langle r_i| \otimes |r_j\rangle\langle r_j| \end{aligned} \tag{10}$$

where Δ_i^{hf} and Δ_i^r are the site-specific detunings of the driving laser fields from the coupling frequency of $|0\rangle \rightarrow |1\rangle$ and $|1\rangle \rightarrow |r\rangle$ respectively. For the Rydberg interaction term $|r_i\rangle\langle r_i| \otimes |r_j\rangle\langle r_j| = \hat{n}_i\hat{n}_j = |r_j\rangle\langle r_j|$ is the number operator which equals 1 if the atom is in $|r_j\rangle$ and 0 otherwise, and

$$V_{ij} = \frac{C_6}{|\vec{x}_j - \vec{x}_k|^6}. \tag{11}$$

C. Nonlinear Susceptibility

Now that we have addressed the phenomena of EIT and Rydberg interactions, we can examine the nonlinearities that emerge from each effect. We begin by solving the master equations for a single atom in a 'L' type configuration to obtain an expression for the nonlinear susceptibility of our system. The full derivation can be found in [1], which follows the method of [8, 23]. The master equations for our configuration are:

$$\begin{aligned} \dot{\rho}_{10} &= -i\frac{\Omega_{hf}}{2}(\rho_{00} - \rho_{11}) + i\delta\rho_{10} - i\frac{\Omega_r}{2}\rho_{r0} - \gamma_{10}\rho_{10} \\ \dot{\rho_{r0}} &= i\frac{\Omega_{hf}}{2}\rho_{r1} + i(\delta + \Delta)\rho_{r0} - i\frac{\Omega_r}{2}\rho_{10} - \gamma_{r0}\rho_{r0} \\ \dot{\rho}_{r1} &= -i\frac{\Omega_r}{2}(\rho_{11} - \rho_{rr}) + i\Delta\rho_{r1} + i\frac{\Omega_{hf}}{2}\rho_{r0} - \gamma_{r1}\rho_{r1}, \end{aligned} \tag{12}$$

where γ_{ij} are the decoherence rates of driven transitions from energy levels $i \leftrightarrow j$. Solving this system of equations in the weak-probe limit with populations $\rho_{00} = 1, \rho_{11} = 0, \rho_{rr} = 0$ gives:

$$\begin{aligned} \rho_{10} &= -\frac{i\Omega_{hf}/2}{\gamma_{10} - i\delta + \Omega_r^2/[\gamma_{r0} - i(\delta + \Delta_]/4} \\ \rho_{r0} &= -\frac{i\Omega_r/2}{\gamma_{r0} - i(\delta + \Delta)}\rho_{10} \\ \rho_{r1} &= 0. \end{aligned} \tag{13}$$

We can then write our electrical susceptibility for our three-level 'L' setup [1]. Note that χ_3 and χ_2 here do not refer to the order of the nonlinear suspectibility, but to the number of allowed states in the setup.

$$\chi_3 = \chi_2 \left(1 - \frac{\Omega_r^2}{4(\gamma_{r0} - i(\delta + \Delta))(\gamma_{10} - i\delta) + \Omega_r^2}\right), \tag{14}$$

where χ_2 is the susceptibility of a bare two-level system $0 \leftrightarrow 1$ without accessing the Rydberg state given by:

$$\chi_2 = \frac{1}{kl_a}\frac{i\gamma_{10}}{\gamma_{10} - i\delta}. \tag{15}$$

Here k is the wavenumber and l_a is the resonant attenuation length. In the two-photon resonance case we addressed previously (Section II: A), this simplifies to:

$$\chi_{3:two-photon} = \chi_{2:two-photon}\left(1 - \frac{\Omega_r^2}{4\gamma_{r0}\gamma_{10} + \Omega_r^2}\right). \tag{16}$$

Remembering that $\chi_{3:two-photon} \to 0$ is a condition for transparency, we see that such transparency requires $\Omega_r^2 \gg 4\gamma_{r0}\gamma_{10}$. We now re-introduce the EIT transparency window from Figure 2 as the EIT linewidth $\Gamma_{EIT} = \Omega_r^2/4\gamma_{10}$. Assuming that $\Gamma_{EIT} \ll \gamma_{10}$, we obtain:

$$\chi_{3:two-photon} \approx \chi_{2:two-photon}\left(1 - \frac{\Gamma_{EIT}}{\Gamma_{EIT} - i\delta}\right). \tag{17}$$

This in turn provides an equation for the group index if we linearize the susceptibility around $\Delta = 0$ and take the real portion $\chi_r \approx \Delta/(\Gamma_{EIT} k l_a)$

$$n_g \approx \frac{\omega}{2}\frac{\partial \chi_r}{\partial \delta} \approx \frac{1}{kl_a}\frac{\omega}{2\Gamma_{EIT}}. \tag{18}$$

This equation reveals that a narrow EIT linewidth directly increases a large group index. In other words, transparency is best achieved by systems that minimize Γ_{EIT}. To do this while maintaining $\Gamma_{EIT} \gg \gamma_{r0}$ we must have $|r\rangle$ be a long-lived state, which is indeed the case for the Rydberg state $100S_{1/2}$. However the Rydberg state brings with it the Rydberg interaction, which we have not included in our master equations. We now address the nonlinear effect of Rydberg blockade.

The Rydberg blockade effect changes the susceptibility of atoms neighboring an $|r\rangle$-state atom from a three-level χ_3 to a two-level χ_2. This is a natural consequence of the $|r\rangle$-state being forbidden to any atom within the blockade radius r_b, as previously three-level atoms can now only access two states. The classical Rydberg non-linearity, then, can be written as [24]:

$$\chi^{(3)} = N\frac{4\pi}{3}r_b^3\frac{\Omega_h f^2}{\Omega_r^2}\chi_2, \tag{19}$$

where N is the atomic density. We can now combine our knowledge of the Rydberg blockade effect with the above derivation of the EIT linewidth to derive [1] a more formal equation for the blockade radius.

$$r_b = \sqrt[6]{C_6/(2\hbar\Gamma_{EIT})} \tag{20}$$

As we saw in the previous section, this blockade radius can be as large as $11\mu m$. Considering that the nonlinear effect of our Rydberg blockade will only increase with the number of blockaded atoms, this means that we can use Rydberg blockade to enhance the nonlinearities of conventional EIT materials [8]. At the single-photon scale, this means the transmission amplitude for photons shone onto the blockade sphere created by an excited atom is [25]:

$$t_2(\delta) = \exp -\frac{\gamma_{10}}{\gamma_{10} - i\delta}\frac{r_b}{l_a} \tag{21}$$

The above treatment reveals that the transmission of photons through a blockaded region can be tuned experimentally. In other words, a configuration of Rydberg atoms can be made reflective, transparent, or partially transparent to incoming resonant light.

III. ATOMIC ENSEMBLES

We will now discuss how nonlinearities emerge in collections of Rydberg atoms. Starting from Rydberg superatoms, we will see how collective addressing of a Rydberg atom ensemble can generate single photons, create metasurfaces, and generate highly entangled photon states for applications in atomic control and quantum information.

A. Rydberg Superatoms

We have established that only a single Rydberg atom is allowed within the blockade radius. However, this does not mean that a cloud of atoms within r_b must have a single pre-determined excitation. If a cloud of atoms is addressed collectively the single Rydberg excitation can be distributed with equal probability across all atoms in the cloud. This idea was first proposed by Lukin and collaborators in 2001 [2], and it effectively allows us to consider the two allowed states of an atomic ensemble (An unexcited ground state and collectively addressed

excited state) as a two-level atom. This two-level structure is commonly referred to as a Rydberg superatom [5–7].

Some interesting features of Rydberg superatoms are increased excitation and emission rates as compared to individual Rydberg atoms. We will simply state the results here, but a full derivation of these rates is found in [6]. Consider a three-level atom with an 'L' structure. The Hamiltonian for many such atoms interacting through the Rydberg interaction is written in Equation 10. The ground state of this Hamiltonian has each individual atom at the lowest ground state $|0\rangle$, which we can write for N atoms as [6]:

$$|G\rangle = |g_1, g_2, ..., g_N\rangle. \tag{22}$$

Note that our Hamiltonian can be adapted to any arbitrary configuration of atoms in free space. Applying the constraint that the spatial distribution of these atoms is confined within a sphere of radius r_b, we can then write the excited state of this ensemble as [6]:

$$|W\rangle = \frac{1}{\sqrt{N}} \sum_j e^{ik' \cdot r_j} |g_1, ..., r_j, ..., g_N\rangle, \tag{23}$$

where $k' = k_0 + k_1 - k_r$ (k_0, k_1, k_r are the wave vectors of the drive fields) and r_j denotes an atom at index j in the Rydberg state. We will call this the collective bright state [6]. Calculating the coupling strength of the atomic ensemble to an external light field (initially filled with a single photon),

$$\langle 0|\langle W|H(t)|G\rangle|1_{k_0}\rangle = \sqrt{N}\hbar g_0, \tag{24}$$

reveals that the coupling strength of N atoms to a single photon is enhanced by a factor of $\sqrt{N}$ as compared to a single atom's coupling to a single photon. This enhances the emission and decay processes of the atom by a factor of N [6]. Upon calculation of the spontaneous emission of $|W\rangle$ it is also found that the final state of our system (the atomic ensemble and light field) is preferred to be [7]:

$$|W \to \psi\rangle = |g_1, g_2, ..., g_N\rangle \otimes |1_{k_0}\rangle. \tag{25}$$

This means that a Rydberg superatom can be used as a single-photon source, and indeed such a source has been realized experimentally [4] with an average photon production rate of $1.18(2) \cdot 10^4$ photons per second. The scheme is as follows. After an excitation of the ground state $|G\rangle$ into an excited state $|W\rangle$ by a resonant π-pulse on resonance with the $|1\rangle \to |r\rangle$ transition, spontaneous emission from the excited state would make the superatom emit a single photon. Continuous excitation and spontaneous emissions from this setup would then act as a single photon source. The rate of single photon generation would be set by the spontaneous emission rate of $|W\rangle$, which is amplified by a factor of N. While this factor of N suggests that the rate of spontaneous emission and thus single photon generation is maximized at highest atomic density, experimental limitations, decoherence and thermal noise limit realizable values of N [7].

B. Engineering Metasurfaces

With our superatom being a two-level system with states $|G\rangle, |W\rangle$, it is possible to initialize our superatom to be in a superposition of these two states. This idea is formalized in [3], where Lukin et al. propose a quantum metasurface composed of atoms placed less than one wavelength of driving light apart in a 2D array (Figure 4). Due to the sub-wavelength spacing this array can act as a mirror with near-perfect reflectivity.

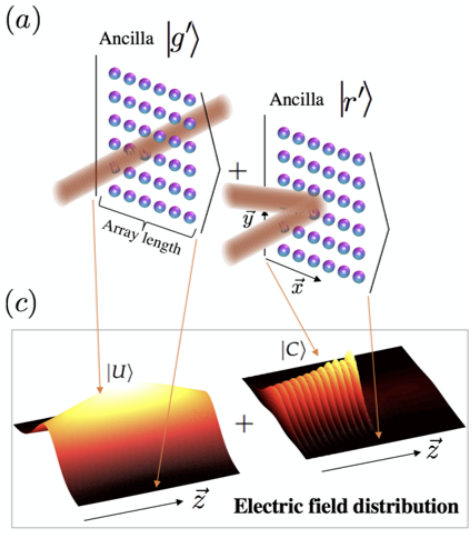

FIG. 4. Figure from [3]. **Top (a):** Diagram illustrates scattering from an array of Rydberg atoms at sub-wavelength spacing (quantum metasurface) that perfectly reflects coupled light and perfectly transmits uncoupled light tuned resonant to $|g\rangle \to |e\rangle$. **Bottom (c):** Numerical plots of the electric field distribution post-scattering of light off the metasurface.

By preparing the array in a superposition of $|G\rangle$ and $|W\rangle$, which correspond to two very different nonlinear susceptibilities, the transmission and reflection of the array would become a source of entanglement for any photon close to resonance sent towards the array. To make this clearer, the authors provide the example of an atomic array initially in the cat state $|\psi_{atom}\rangle = \frac{1}{\sqrt{2}}(|G\rangle + |W\rangle)$. Upon interaction with a right propagating coherent light wave $\psi_{photon} = |\alpha, 0\rangle$ (The first entry corresponds to a right propagating mode of light, the second entry to a left propagating mode) perpendicular to the array, the post-scattering state of the entire system is:

$$|\psi_{system}\rangle = \frac{1}{\sqrt{2}}(|G\rangle \otimes |\alpha, 0\rangle + |W\rangle \otimes |t\alpha, r\alpha\rangle), \tag{26}$$

where r and t are the reflection and transmission coefficients of the atomic array. When $t \to 0$ is achieved by driving with light tuned to the cooperative resonance of the entire array, the system state is then:

$$|\psi_{system}\rangle = \frac{1}{\sqrt{2}}(|G\rangle \otimes |\alpha, 0\rangle + |W\rangle \otimes |0, -\alpha\rangle). \tag{27}$$

Intriguingly, a projective measurement of $|\psi_{system}\rangle$ in the basis of input cat states $\frac{1}{\sqrt{2}}(|G\rangle \pm |W\rangle)$ of the atomic array projects the scattered light into the photonic cat states $|\psi_{photons}\rangle = \frac{1}{\sqrt{2}}(|\alpha, 0\rangle \pm |0, -\alpha\rangle)$. In other words, this POVM has disentangled the atomic array from the state of our output photons and left a two-photon Bell state. This scheme can be expanded to create GHZ states for n photons of form [3]:

$$|\psi_{photons}\rangle_n = \frac{|01\rangle^{\otimes n} + |10\rangle^{\otimes n}}{\sqrt{2}}. \tag{28}$$

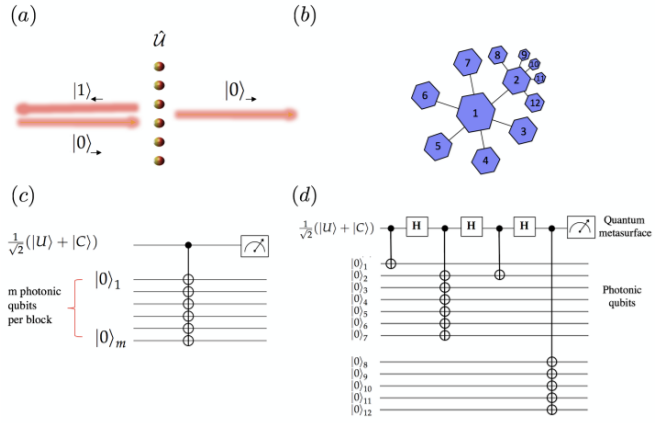

FIG. 5. Figure from [3]. Schematic for photonic GHZ state preparation. (a) Cartoon that shows how only photons of the correct propagation $|0\rangle$ can transfer through the metasurface. (b) Graph of a highly entangled state analogous to the GHZ state. (c) Measurement circuit for a photonic GHZ state. This disentangles the atomic ensemble. (d) Quantum circuit for the preparation of an n photon GHZ state. H represents Hadamard gate.

The circuitization of this method is found in Figure 5, and the described method for GHZ state generation has been used experimentally to create a GHZ state of 12 photons [5]. More complicated states and even quantum circuits can be created by selectively tuning the transmittance of the Rydberg atom array. In general, controlled multiqubit gates of form are possible:

$$U = \sum_{\phi} |\phi\rangle\langle\phi| \otimes_k V_{k,\phi}, \tag{29}$$

where $V_{k,\phi}$ is some unitary with components correlating to the transmittance scattering coefficients. And as a Hadamard gate and CNOT can be performed, this is already enough to form a universal gate set [7]. In theory, this means that one could use Rydberg atom arrays as nonlinear beamsplitters in an all-optical quantum computer. While it would not be ideal to run circuits involving a large depth of quantum gates on this all-optical setup due to the photon state's entanglement with the state of the atomic array, the near perfect reflectivity and tunable transmittance of Rydberg atom arrays could make them great beamsplitters.

IV. CONCLUSION

Highly entangled photon states, single photon sources, and atomic ensembles with high nonlinear susceptibilities are but a few examples of the nonlinear effects that emerge from EIT and Rydberg blockade. Other applications not touched on in this paper include the demonstration of quantum gates using EIT [10], extensions of the photon entanglement scheme discussed here to perform quantum logic gates for two optical photons [26], optical switches to alter the transmission of a target photon based on the outcome of a control photon [27], and coherent interactions between two photons traveling through a Rydberg atom ensemble [15]. For further readings on EIT and Rydberg atom ensembles that provide a comprehensive introduction to these topics, we strongly recommend a review of EIT (Fleischhauer et al. [8]), a review of nonlinear quantum optics from Rydberg interactions (Firstenberg et al. [1]), and a more general review of quantum information with Rydberg atoms (Saffman et al. [7]).

[1] C. A. O Firstenberg and S. Hofferberth, Journal of Physics B: Atomic Molecular and Optical Physics **49** (2016).
[2] R. C. L. M. D. D. J. J. I. C. M. D. Lukin, M. Fleischhauer and P. Zoller, Phys. Rev. Lett. **87** (2001).
[3] H. P. E. S. S. F. Y. Rivka Bekenstein, Igor Pikovski and M. D. Lukin, OSA Quantum 2.0 Conference (2020).
[4] E. A. G. A. J. H. Y. W. P. B. A. V. G. S. L. R. D. P. Ornelas-Huerta, A. N. Craddock and J. V. Porto, Optica **7** (2020).
[5] J. L. B. J. X.-H. B. Chao-Wei Yang, Yong Yu and J.-W. Pan, Nature Photonics **16** (2022).
[6] C. T. N. S. S. H. Jan Kumlin, Christoph Braun and A. Pairs-Mandoki, J. Phys. Commun. **7** (2023).
[7] T. G. W. M. Saffman and K. Mølmer, Rev. Mod. Phys. **82** (2010).
[8] A. I. Michael Fleischhauer and J. P. Marangos, Reviews of Modern Physics **77** (2005).
[9] J. Vanier, Applied Phys. B **81** (2005).
[10] L. K. K. McDonnell and J. Pritchard, Phys. Rev. Lett. **129** (2022).
[11] X. W. P. Z. Zhao and D. Tong, Phys. Rev. A **98** (2018).
[12] S. B. C. M. J. J.-D. H. S. Yuqi Zhu, Sumita Ghosh and R. H. Maruyama, Phys. Rev. A **105** (2022).
[13] T. P. M. A. A. H. Safavi-Naeini and O. Painter, Nature **472** (2011).
[14] P. B. Krzysztof Jachymski and H. P. Büchler, Phys. Rev. Lett. **117** (2016).

[15] Q.-Y. L. A. V. G.-M. D. L. Ofer Firstenberg, Thibault Peyronel and V. Vuletić, Nature **502** (2013).
[16] A. A. G. S. H. L. H. Z. T. M. S. E. M. C. M. K. D. H. J. P. B. A. N. M. I. C. X. G. P. S. R. T. K. G. S. M. J. G. M. G. V. V. Dolev Bluvstein, Simon J. Evered and M. D. Lukin, Nature **626** (2024).
[17] P. P. B. Z. S. J. J. C. A. P. B. G. P. S. P. Shuo Ma, Genyue Liu and J. D. Thompson, Nature **622** (2023).
[18] J. H. E. Haller and S. Kuhr, Nature Physics **11** (2015).
[19] J. Kim, Duke University (2020).
[20] C. Genes, Florida Atlantic University (2019).
[21] A. I. K.J. Boller and S. E. Harris, Phys. Rev. Lett. **66** (1991).
[22] X. Shi, Quantum Sci. Technol. **7** (2022).
[23] S.-z. J. Julio Gea-Banacloche, Yong-qing Li and M. Xiao, Phys. Rev. A **51** (1995).
[24] C. A. S. Sevinçli, N. Henkel and T. Pohl, Phys. Rev. Lett. **107** (2011).
[25] M. F.-T. P. Alexey V. Gorshkov, Johannes Otterbach and M. D. Lukin, Phys. Rev. Lett. **107** (2011).
[26] M. W. B. R. Y.-F. H. L. H. G. R. Thomas Stolz, Hendrik Hegels and S. Dürr, Phys. Rev. X **12** (2022).
[27] G. R. Simon Baur, Daniel Tiarks and S. Dürr, Phys. Rev. Lett. **112** (2014).